nature nanotechnology

LETTERS

PUBLISHED ONLINE: 6 APRIL 2014 | DOI: 10.1038/NNANO.2014.58

Universal computing by DNA origami robots in a living animal

Yaniv Amir[1†], Eldad Ben-Ishay[1†], Daniel Levner[2], Shmulik Ittah[1], Almogit Abu-Horowitz[1] and Ido Bachelet[1*]

Biological systems are collections of discrete molecular objects that move around and collide with each other. Cells carry out elaborate processes by precisely controlling these collisions, but developing artificial machines that can interface with and control such interactions remains a significant challenge. DNA is a natural substrate for computing and has been used to implement a diverse set of mathematical problems[1–3], logic circuits[4–6] and robotics[7–9]. The molecule also interfaces naturally with living systems, and different forms of DNA-based biocomputing have already been demonstrated[10–13]. Here, we show that DNA origami[14–16] can be used to fabricate nanoscale robots that are capable of dynamically interacting with each other[17,18] in a living animal. The interactions generate logical outputs, which are relayed to switch molecular payloads on or off. As a proof of principle, we use the system to create architectures that emulate various logic gates (AND, OR, XOR, NAND, NOT, CNOT and a half adder). Following an *ex vivo* prototyping phase, we successfully used the DNA origami robots in living cockroaches (*Blaberus discoidalis*) to control a molecule that targets their cells.

To implement a collision-based computer using DNA objects, we used DNA origami nanorobots as described previously[19] (Supplementary Note 1). These robots are controlled by a gate that opens in response to a correct combination of protein cues, which bind a sensing strand, typically an aptamer, and displace it from its complementary strand. Upon displacing the gate strands from each other, the robot undergoes a drastic conformational shift, exposing the payload inside it and making it available to engage target cells.

In the present design, the gate can also be opened by an external DNA key, which hybridizes with the complementary strand in the gate, displacing the sensing strand by toehold-mediated migration[17,18] and activating the robot. This DNA key can now be mounted as a payload into one robot such that when this robot is active, the strand can access the gate of an adjacent robot, subsequently altering its state to active as well. This assigns a 'positive regulator' (P) phenotype to the robot loaded with the external key. A 'negative regulator' (N) phenotype can also be assigned, where the first robot is loaded with DNA clasps that crosslink two juxtaposed sides of the second robot's gate, forcing it to close or preventing it from becoming open. These dynamic DNA interactions were designed and simulated using visual DNA strand displacement (DSD)[20] (Supplementary Note 2).

We designed various architectures by mixing P and N robots with effector (E) robots at defined ratios, in the presence or absence of their cognate protein cues. To demonstrate this platform in a living biological system, we used living adult *Blaberus discoidalis* as model organisms. We found this animal to be an excellent model for the initial prototyping of DNA nanodevices because of its very low systemic nuclease activity, small systemic volume and chemical compatibility with DNA structures. After loading E robots with an antibody recognizing the insect's haemocytes (haemolymph cells, analogous to human white blood cells), robot mixtures were tested on freshly isolated haemocytes and then injected into the living animals (Supplementary Notes 3 and 4).

We first tested E robots controlled by a gate that opens if and only if both cues (termed X and Y) are present. E robots alone (which we call an E architecture) emulate a logical AND gate (Fig. 1a, Supplementary Fig. 15), as previously described[19]. We next added two robot types, P1 (opens in response to X and carries a single key to the Y gate of E) and P2 (opens in response to Y and carries a single key to the X gate of E). Adding P1 and P2 to E (EP1P2 architecture) enables E to open in response to X alone (by P1), Y alone (by P2) or XY (by itself), emulating a logical OR gate (Fig. 1a, Supplementary Fig. 16). Binding of target cells by an EP1 or EP2 robot complex instead of just E robots was shown by tagging P1 and P2 with fluorophores, resulting in fluorescence intensity patterns clearly indicating the presence of EP complexes (Supplementary Fig. 17). It is important to note that an OR gate can be achieved more simply using one or two robot types. However, three robots have a higher capacity for molecular control (three therapeutic molecules instead of two). We observed no significant change in speed or error rate when moving from two to three robots in this configuration.

We then added N robots (EP1P2N architecture), N being activated if and only if both X and Y are present. Here, in contrast to EP1P2, the presence of both X and Y activates N, which carries multiple clasp arms that close E, subsequently negating or preventing E activation (importantly, the N clasps cannot hybridize with the N gates themselves). These outputs are identical to those generated by an XOR gate. In the final state of the EP1P2N architecture, E is always in complex with P1 or P2 (when it is active) or N (when it is inactive). XOR was successfully emulated only when N was at a molar excess of 10 over E (Fig. 1a, Supplementary Fig. 18).

E robots in EP1P2N generate XOR, while N robots in this architecture generate AND, together enabling the construction of a half adder, in which the sum bit is relayed by E and the carry bit by N. Hence, it can be programmed to respond to a cue count rather than to the identity of particular cues. However, both robot types in the EN complex (unlike in the EP complexes) directly face each other, so utilizing N to deliver a payload is sterically inhibited. However, the carry bit can be relayed by adding a second effector robot (F), which is not keyed by P1 and P2 and is not negated by N. Thus, either X or Y alone activate E, while XY together activate

[1]Faculty of Life Sciences and the Institute of Nanotechnology & Advanced Materials, Bar-Ilan University, Ramat Gan 52900, Israel, [2]Wyss Institute for Bio-Inspired Engineering, Harvard Medical School, 3 Blackfan Circle, Boston, Massachusetts 02115, USA. †These authors contributed equally to this work. *e-mail: ido.bachelet@biu.ac.il

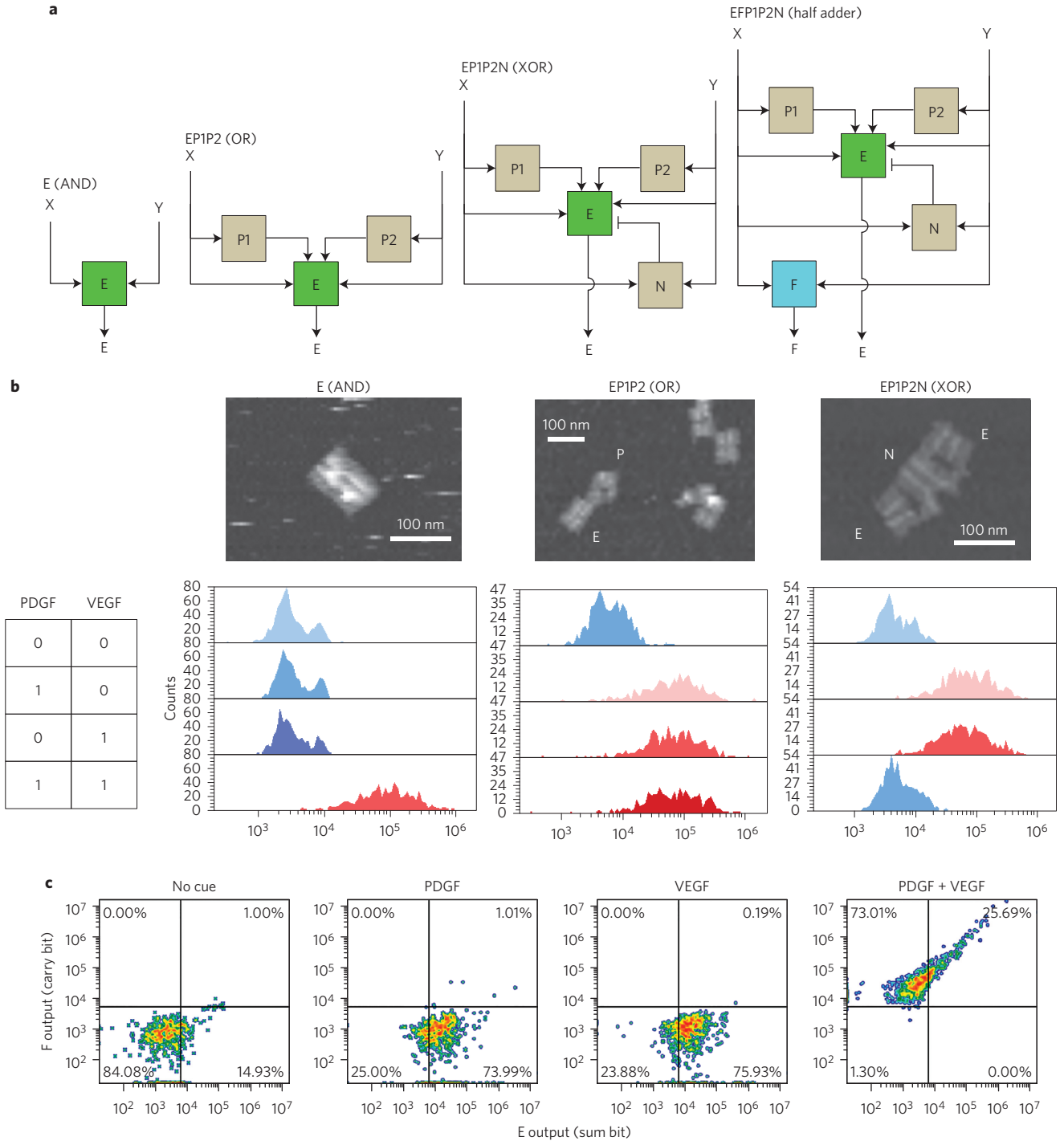

Figure 1 | Robots emulating AND, OR, XOR gates and a half adder in a living animal. a, Schematic architecture representations. E robots (leftmost) are equivalent to an AND gate, requiring both X and Y (in this study platelet derived growth factor (PDGF) and vascular endothelial growth factor (VEGF), respectively) to open. The EP1P2 architecture (second from left) functions as an OR gate, requiring either X, Y or both to open. The EP1P2N architecture (third from left) functions as an XOR gate, opening with either X or Y, but closing with both X and Y. EFP1P2N (right) emulates a half adder encoding the sum bit in E and carry bit in F. **b**, Top: Atomic force microscope images of robot architectures. Below each image are corresponding flow cytometric analyses of insect cells isolated from *B. discoidalis* several hours following the injection of robots and appropriate keys. The table shows the key combinations corresponding to each row in the histograms. E robots (FL1 channel) were tagged with fluorescein amidite (FAM). Blue/red peaks represent negative/positive signals, respectively. **c**, Flow cytometric analysis of the EFP1P2N architecture, emulating a half adder. E robots representing the sum bit (FL1 channel) and F robots (FL4 channel) representing the carry bit of the half adder were measured simultaneously *in vivo* using FAM and Cy5 tagged robots. A total of 1,000 haemocytes were collected for each experiment.

only F (E being negated by N). P1 and P2 cannot key F because the toeholds extending from the F gates are different from those on the E gates. Moreover, N cannot negate F, because F gates lack the additional extensions that enable N arms to clasp them together (Supplementary Note 2). The half adder (EFP1P2N) functioned well at a stoichiometry of 1:1:5:5:10 (Fig. 1a,c). This stoichiometric

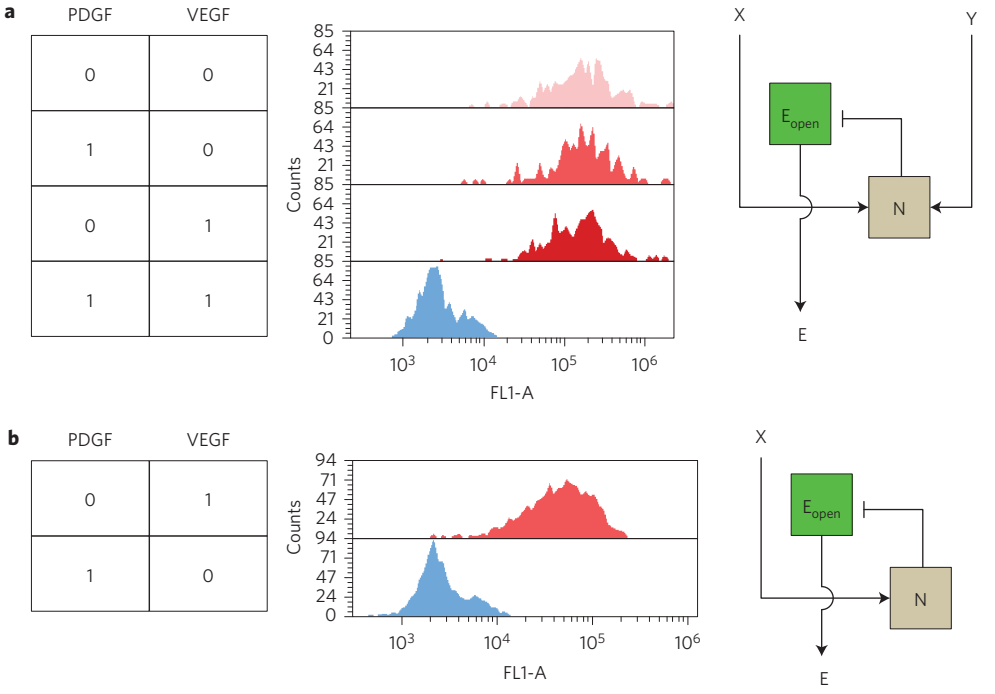

Figure 2 | Robots emulating NAND and NOT gates in a living animal. a, $E_{open}N$ architecture emulating the logically complete NAND gate. **b**, $E_{open}N_X$ architecture emulating an inverter (NOT). Histograms are flow cytometric analyses of haemocytes extracted from *B. discoidalis* following injection of the proper robot architectures with keys. The tables show key profiles corresponding to each row in the histograms. Also shown are schematic representations of robot architectures. A total of 1,000 haemocytes were collected for each experiment.

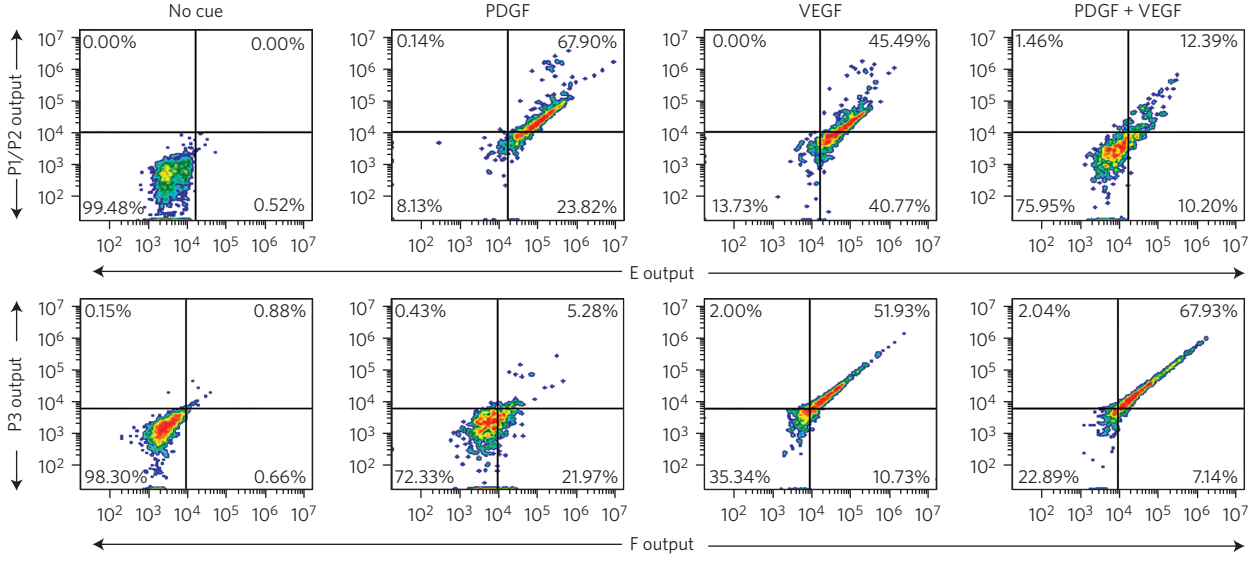

Figure 3 | Robots emulating the reversible CNOT gate in a living animal. Flow cytometric analysis of *B. discoidalis* cells extracted following injection of the EFP1P2P3N architecture with various key profiles. E robots (FAM-tagged, FL1) and P1/P2 robots (Cy5-tagged, FL4) represent the state of the first bit entering the gate; F robots (Alexa546-tagged, FL2) and P3 robots (Alexa594-tagged, FL3) represent the state of the second bit, which remains unchanged. Slanting patterns of double-positive labelled cells indicate the presence of EP and FP complexes (Supplementary Fig. 17). A total of 1,000 haemocytes were collected for each experiment.

hierarchy was highly consistent with the predictions made in vDSD as to the EP and EPN collisions.

We introduced a modified type of E, termed E_{open}, which is similar to E but lacks sensing strands (thus it is constitutively open regardless of inputs X and Y). The $E_{open}N$ architecture, made by mixing E_{open} with N, produces 0 in response to XY and 1 otherwise, like the NAND gate (Fig. 2a, Supplementary Fig. 19). An inverter (NOT) can be readily designed as a variant of the NAND gate, constructed by programming N to respond only to X (by placing two identical X gates instead of X and Y gates on the robot), termed N_X. The E_{open}:N_X architecture produces 1 if X is absent (by E_{open}) and 0 if X is present (by N_X negating E_{open}) (Fig. 2b).

Architectures based on more than one effector robot (like the EFP1P2N mentioned above) can relay output bits to additional therapeutic molecules, forming the basis for more complex gates, reversible logic and binary decoders. To demonstrate this, a controlled NOT

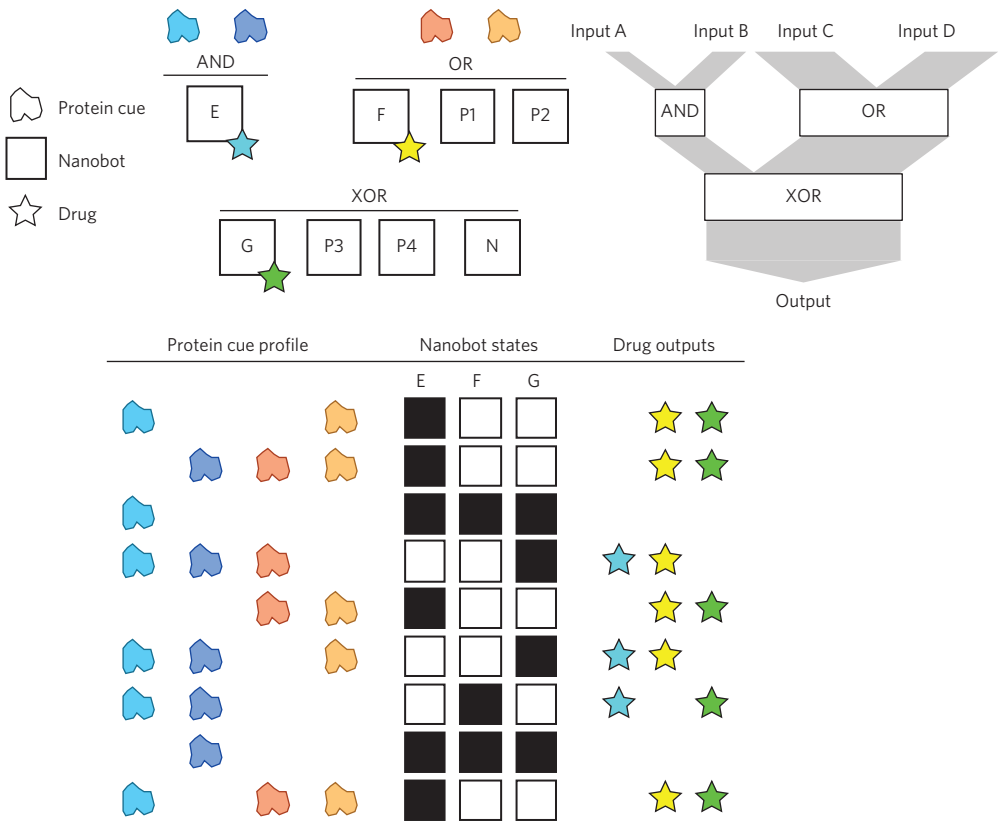

Figure 4 | A hypothetical system capable of simultaneously controlling three therapeutic molecules. This system serves as a processor for an imaginary medical task where a therapeutic response should be tailored to each disease state from a selection of three drugs. The system consists of eight robot types: three effector robots E, F and G, each carrying a different drug; four positive regulators, P1 and P2 keying F, P3 and P4 keying G; and a negative regulator N inactivating G. Together they form two first-layer gates, AND and OR, each controlling its own drug while relaying its output state to a second-layer XOR gate, which controls a third drug. This example lists four distinct drug combination outputs that could be generated by this system.

(CNOT) gate was designed, consisting of E, P1, P2 and N as described above, as well as a second effector robot, F, not negated by N, and a positive regulator robot P3 that responds only to X and keys only F. Thus, one input bit is XORed by E, and the second input bit is mapped unchanged by F. The CNOT gate (EFP1P2P3N) functioned well at a 1:1:5:5:5:10 stoichiometry (Fig. 3; see also Supplementary Table 1 for a summary of the outputs and effector complexes in the various architectures designed in this study).

The performance of our system and similar ones depends on the ability of its parts to interact freely. We used fluorescence correlation spectroscopy to measure robot diffusion in a medium mimicking the fluid mechanical properties of the insect's haemolymph (Supplementary Note 5, Supplementary Fig. 26), yielding a diffusion coefficient of $19 \pm 1.1\ \mu^2\ s^{-1}$ for the open state and $21 \pm 2.6\ \mu^2\ s^{-1}$ for the closed state. Typically, 0.1–3 pmol robots interact within an average haemolymph volume of 650 µl (assuming total cell volume is negligible). While in this space and medium sheer diffusion would probably not support efficient collisions in reasonable timescales (Supplementary Fig. 27), the insect haemolymph is constantly mixed. *Periplaneta americana*, closely related to *B. discoidalis*, has a heart rate of 130 ± 10 beats/min with an average stroke volume of 1.9 ± 0.31 µl, resulting in a cardiac output equivalent to 38% of the haemolymph volume per minute, providing for efficient computing as observed here. The estimated Reynolds number of the insect's open circulatory system is on the order of 1–5 due to the low-velocity flow within the small haemocoel[21]. Compared to that, Reynolds numbers in the human circulatory system range from 1 in arterioles to ~4,000 in the aorta and vena cava. Therefore, our study shows that computing in human blood should be at least as efficient as that observed in the insect model. Scaling the system to humans would require increasing the robot quantity by approximately four orders of magnitude and constructing them using nuclease-resistant analogues such as locked nucleic acid (LNA). These essentially technical issues should be achievable in the very near future.

The architectures described here are capable of processing two input bits at most. However, the outputs from two 'processors' can be relayed to a third and increase the processing capacity (limited by the possible number of unique gate-key systems that can be designed). Importantly, the scaling of our design is linear rather than logarithmic, with errors in robot activation propagating in the order of the root sum square of the number of unique robot types in a system (Supplementary Note 6). Figure 4 presents a schematic of a hypothetical 4-input bit architecture for an imaginary task of controlling three therapeutic molecules simultaneously, where only the number of robots comprising the system limits its capacity. The basic concept we describe can be scaled plausibly to exceed the capacity of older 8-bit computers such as a Commodore 64 or Atari 800, which many of us had experience of as children.

The system we describe can also be used to retrieve biochemical and physiological information as a diagnostic tool. However, for this, the original cues need to be explicitly inferred from the final states of all the robots comprising the system. This is not possible in gates such as AND, OR and XOR, as these lose 1 bit per operation. However, it is made possible in reversible logic[22], using operators such as the CNOT gate demonstrated here, in which every input bit is mapped to an output bit. This information could be analysed in various ways, for example, by monitoring fluorescent outputs associated with robot final states.

This work presents a new type of biological computing platform particularly fit for the task of controlling therapeutic molecules in living organisms. Further design work building on this concept could significantly improve the capacity and efficiency of such systems with a view to developing a working prototype for computational control of therapeutics and other biological processes in humans in the near future.

Methods

DNA origami robots were designed using caDNAno 2.0 (http://caDNAno.org), and folded using M13mp18 ssDNA as the scaffold strand in TAE buffer containing 10 mM magnesium. Robots were cleaned by gel filtration on Amicon Ultra 100K columns. DNA strand displacement interactions were designed and simulated using visual DSD. Robots were imaged using transmission electron microscopy and atomic force microscopy and their states were measured using flow cytometry. Adult *B. discoidalis* were maintained at constant room temperature in humid plastic cages with dry pet food and fresh fruit *ad libitum*. Robots (typically 0.1–3 pmol in 10 μl buffer) were injected into the animal haemocoel between the two last abdominal sternites. Haemolymph was extracted through the arthrodial membrane and mixed with anticoagulant buffer before haemocyte analysis. For detailed methods see Supplementary Information.

Received 2 October 2013; accepted 21 February 2014; published online 6 April 2014

References

1. Adleman, L. M. Molecular computation of solutions to combinatorial problems. *Science* **266,** 1021–1024 (1994).
2. Braich, R. S., Chelyapov, N., Johnson, C., Rothemund, P. W. & Adleman, L. Solution of a 20-variable 3-SAT problem on a DNA computer. *Science* **296,** 499–502 (2002).
3. Qian, L., Winfree, E. & Bruck, J. Neural network computation with DNA strand displacement cascades. *Nature* **475,** 368–372 (2011).
4. Seelig, G., Soloveichik, D., Zhang, D. Y. & Winfree, E. Enzyme-free nucleic acid logic circuits. *Science* **314,** 1585–1588 (2006).
5. Stojanovic, M. N., Mitchell, T. E. & Stefanovic, D. Deoxyribozyme-based logic gates. *J. Am. Chem. Soc.* **124,** 3555–3561 (2002).
6. Stojanovic, M. N. *et al.* Deoxyribozyme-based ligase logic gates and their initial circuits. *J. Am. Chem. Soc.* **127,** 6914–6915 (2005).
7. Andersen, E. S. *et al.* Self-assembly of a nanoscale DNA box with a controllable lid. *Nature* **459,** 73–76 (2009).
8. Lund, K. *et al.* Molecular robots guided by prescriptive landscapes. *Nature* **465,** 206–210 (2010).
9. Muscat, R. A., Bath, J. & Turberfield, A. J. A programmable molecular robot. *Nano Lett.* **11,** 982–987 (2011).
10. Benenson, Y., Gil, B., Ben-Dor, U., Adar, R. & Shapiro, E. An autonomous molecular computer for logical control of gene expression. *Nature* **429,** 423–429 (2004).
11. Benenson, Y. *et al.* Programmable and autonomous computing machine made of biomolecules. *Nature* **414,** 430–434 (2001).
12. Modi, S., Nizak, C., Surana, S., Halder, S. & Krishnan, Y. Two DNA nano machines map pH changes along intersecting endocytic pathways inside the same cell. *Nature Nanotech.* **8,** 459–467 (2013).
13. Rudchenko, M. *et al.* Autonomous molecular cascades for evaluation of cell surfaces. *Nature Nanotech.* **8,** 580–586 (2013).
14. Douglas, S. M. *et al.* Self-assembly of DNA into nanoscale three-dimensional shapes. *Nature* **459,** 414–418 (2009).
15. Douglas, S. M. *et al.* Rapid prototyping of 3D DNA-origami shapes with caDNAno. *Nucleic Acids Res.* **37,** 5001–5006 (2009).
16. Rothemund, P. W. Folding DNA to create nanoscale shapes and patterns. *Nature* **440,** 297–302 (2006).
17. Zhang, D. Y. & Seelig, G. Dynamic DNA nanotechnology using strand-displacement reactions. *Nature Chem.* **3,** 103–113 (2011).
18. Zhang, D. Y. & Winfree, E. Control of DNA strand displacement kinetics using toehold exchange. *J. Am. Chem. Soc.* **131,** 17303–17314 (2009).
19. Douglas, S. M., Bachelet, I. & Church, G. M. A logic-gated nanorobot for targeted transport of molecular payloads. *Science* **335,** 831–834 (2012).
20. Lakin, M. R., Youssef, S., Polo, F., Emmott, S. & Phillips, A. Visual DSD: a design and analysis tool for DNA strand displacement systems. *Bioinformatics* **27,** 3211–3213 (2011).
21. Lee, W. K. & Socha, J. J. Direct visualization of hemolymph flow in the heart of a grasshopper (*S. americana*). *BMC Physiol.* **9,** 2 (2009).
22. Liu, D. *et al.* Resettable, multi-readout logic gates based on controllably reversible aggregation of gold nanoparticles. *Angew. Chem. Int. Ed.* **50,** 4103–4107 (2011).

Acknowledgements

The authors thank the following colleagues for their valuable advice and comments on the manuscript: A. Adamatzky, S. Revzen, D.Y. Zhang, R. Jungmann, P. Yin, A. Marblestone, E. Shapiro, A. Munitz, A. Binshtok, L. Qian, E. Winfree and G.M. Church. The authors are particularly grateful to S.M. Douglas for valuable contributions. The authors acknowledge the members of the Bachelet lab at Bar Ilan University for support, technical help and valuable discussions. This work was supported by a European Research Council Starting grant (no. 335332) to I.B., a Kamin grant from the Israeli Ministry of Industry & Commerce to I.B. and grants from the Faculty of Life Sciences and the Institute of Nanotechnology & Advanced Materials at Bar-Ilan University.

Author contributions

All authors designed the experiments. Y.A., E.B.I, S.I., A.A.H. and I.B. performed experiments. All authors contributed to writing the manuscript.

Additional information

Supplementary information is available in the online version of the paper. Reprints and permissions information is available online at www.nature.com/reprints. Correspondence and requests for materials should be addressed to I.B.

Competing financial interests

The authors declare no competing financial interests.